



## Air mass classification in coastal New England and its relationship to meteorological conditions

Ming Chen,<sup>1</sup> Robert Talbot,<sup>1</sup> Huiting Mao,<sup>1</sup> Barkley Sive,<sup>1</sup> Jianjun Chen,<sup>1</sup> and Robert J. Griffin<sup>1,2</sup>

Received 23 June 2006; revised 26 January 2007; accepted 30 March 2007; published 11 May 2007.

[1] The dominant air mass types along coastal New England during summer 2004 were classified and their relationship to synoptic meteorological conditions investigated as a component of the International Consortium for Atmospheric Research on Transport and Transformation (ICARTT) campaign. Representative air mass types were defined on the basis of variability in the occurrence of volatile organic compounds (VOCs), and they were further grouped into distinct source-related categories. Emissions from nearby anthropogenic sources were found to govern the total variance of the data set (58% at Appledore Island (AI) and 56% at Thompson Farm (TF)), whereas long-distance transport was much less dominant (15% on AI and 17% at TF). This result indicates frequent influence from recent anthropogenic emissions at TF and AI, with periodic inputs of aged/processed pollutants. The fractional time periods dominated by anthropogenic (recent and aged/processed) and marine biogenic air masses were almost the same at TF and AI (36% versus 30% and 14% versus 16% respectively), clearly showing the strong impact of continental outflow on the nearshore marine atmosphere and a surprising persistent influence of marine biogenic emissions at an inland site. Empirical orthogonal function (EOF) analysis suggested that the most important circulation pattern during summer 2004 was characterized by a low trough positioned along coastal New England, leaving this region under the control of northwesterly flow from central Canada. This result helps explain why New England in summer 2004 was less polluted compared to previous years.

**Citation:** Chen, M., R. Talbot, H. Mao, B. Sive, J. Chen, and R. J. Griffin (2007), Air mass classification in coastal New England and its relationship to meteorological conditions, *J. Geophys. Res.*, 112, D10S05, doi:10.1029/2006JD007687.

### 1. Introduction

[2] Rural areas in New England often experience high levels of air pollution as a result of transport of urban emissions to the region with additional in situ chemical production of ozone (O<sub>3</sub>) and aerosols during transit [Goldan *et al.*, 2004; Seaman and Michelson, 2000; Moody *et al.*, 1996]. The occurrence of high pollution events in New England was found to be closely associated with meteorological conditions that favor long-range transport from the Midwest and northeast urban/industrial corridor [Ray *et al.*, 1996]. In their high O<sub>3</sub> episode study, Mao and Talbot [2004] revealed that the O<sub>3</sub>-rich air masses from the greater Boston area contributed to the high levels of O<sub>3</sub> in the New Hampshire coastal region.

[3] During the New England Air Quality Study in 2002 (NEAQS 2002), Griffin *et al.* [2004] found that high mixing ratios of O<sub>3</sub> in southeastern New Hampshire were most

likely a result of processed O<sub>3</sub>-rich air masses transported from upwind source regions rather than local in situ chemical production. Zhou *et al.* [2005] demonstrated that the same area had a significant source of marine derived halocarbons, such as bromoform (CHBr<sub>3</sub>) and dibromomethane (CH<sub>2</sub>Br<sub>2</sub>), derived from the coastal Gulf of Maine.

[4] The composition and transport of North American outflow was investigated during the North Atlantic Regional Experiment in summers 1993 and 1997. Merrill and Moody [1996] found that the warm sector flow ahead of an advancing cold front delivers urban plumes from the east coast of the United States to the Gulf of Maine and subsequently to the Maritime Provinces of Canada. Cooper *et al.* [2001] found that the highest carbon monoxide (CO) and total reactive nitrogen (NO<sub>y</sub>) values in the middle and upper troposphere over the North Atlantic were associated with polluted outflow from New England lifted aloft by the warm conveyor belt.

[5] During a recent large-scale field campaign based in southeastern New Hampshire, the International Consortium for Atmospheric Research on Transport and Transformation (ICARTT, <http://esrl.noaa.gov/csd/ICARTT>), a key emphasis was examination of the chemical signature of North American outflow. For example, Russo [2005] observed a similar distribution of seven C<sub>1</sub>-C<sub>5</sub> alkyl nitrates at two

<sup>1</sup>Climate Change Research Center, Institute for the Study of Earth, Oceans, and Space, University of New Hampshire, Durham, New Hampshire, USA.

<sup>2</sup>Also at Department of Earth Sciences, University of New Hampshire, Durham, New Hampshire, USA.

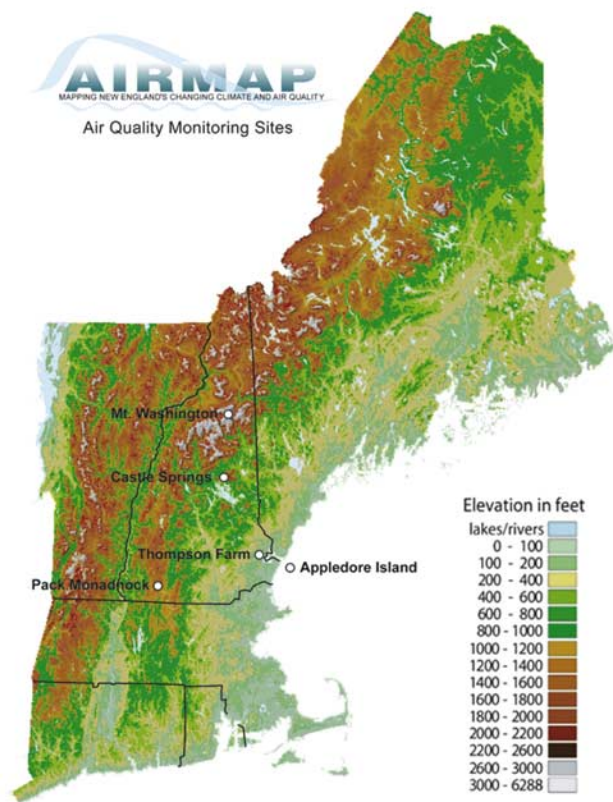


**Figure 1.** Geographic location of Thompson Farm and Appledore Island in eastern New England.

eastern New England AIRMAP sites (<http://www.airmap.unh.edu>) affected consecutively by outflow; one an inland location at Thompson Farm (TF) and the second a Gulf of Maine marine site on Appledore Island (AI). In general, the often higher levels of secondary pollutants at AI compared to TF are related to ongoing photochemical processing in continental outflow. In a study using  $O_3$  measurements obtained from a Lagrangian balloon platform, *Mao et al.* [2006] found that  $O_3$  mixing ratios in continental outflow over the North Atlantic ( $\sim 150$  ppbv) far exceeded the highest mixing ratios from inland sites in New England ( $< 100$  ppbv). Two primary factors appear responsible: (1) effective in situ chemical production inside urban plumes during daytime and (2) strong synoptic transport of  $O_3$  and its precursors, particularly at night.

[6] Previous studies in the northeast have placed a strong emphasis on investigation of multiday episodes of high levels of several specific trace gases. Less attention has been focused on interpreting seasonal variations in a large suite of VOCs and their linkages to source emissions and attendant circulation patterns. In this study, we employed principal component analysis (PCA) to depict commonalities in representative VOCs and used empirical orthogonal function (EOF) to identify associated meteorological variables. The time period of interest spanned 2 July to 15 August 2005 ( $\sim 45$  days) during the central activities of the ICARTT campaign. The two major goals of this study were to (1) identify air mass types and their frequency at TF and AI and (2) determine the relationship between synoptic

circulation patterns and air mass types that caused temporal variations in VOCs levels in eastern New England during summer 2004.

## 2. Measurements and Methods

### 2.1. Field Sites

[7] Measurements of VOCs in ambient air were made at AI and TF located in the coastal New Hampshire area as shown in Figure 1. AI ( $42.97^\circ N$ ,  $70.62^\circ W$ ) is situated 11 km off the coast of New Hampshire in the Gulf of Maine while TF ( $43.11^\circ N$ ,  $70.95^\circ W$ ) resides 20 km inland. The land surface at TF is forested with a mixture of coniferous and deciduous trees. In contrast, AI is covered sparsely by grass and trees.

### 2.2. VOC Measurements at Thompson Farm and Appledore Island During ICARTT

#### 2.2.1. Automated VOC Measurements at Thompson Farm

[8] VOC measurements were conducted at Thompson Farm using an automated gas chromatographic system equipped with two flame ionization detectors and two electron capture detectors [*Sive et al.*, 2005]. During the ICARTT campaign, the system measured a comprehensive suite of  $C_2$ - $C_{10}$  nonmethane hydrocarbons (NMHCs),  $C_1$ - $C_2$  halocarbons and  $C_1$ - $C_5$  alkyl nitrates. Air was drawn from a perfluoroalkoxy (PFA)-Teflon lined manifold at the top of a 12 m tower and subsamples were analyzed every 40 min. Further details regarding the Thompson Farm VOC system are described by *Zhou et al.* [2005].

#### 2.2.2. Canister Samples at Appledore Island

[9] Hourly canister samples were collected at AI from 1 July to 13 August 2004 for  $C_2$ - $C_{10}$  NMHCs,  $C_1$ - $C_2$  halocarbons,  $C_1$ - $C_5$  alkyl nitrates and selected sulfur compounds. Canister samples were collected in 2-liter electropolished stainless steel canisters (University of California, Irvine) and pressurized to 35 psig using a single head metal bellows pump (MB-302MOD, Senior Flexonics, Sharon, Massachusetts). Every 4 days during the summer campaign, canister samples were returned to the laboratory for analysis by gas chromatography using flame ionization and electron capture detection in conjunction with mass spectrometry. Approximately 1032 samples were analyzed during the course of the campaign resulting in a continuous time series of a large suite of VOCs from Appledore Island. Further details of the analytical system are described by *Sive et al.* [2005].

#### 2.2.3. Online VOC Monitoring Using PTR-MS at Thompson Farm and Appledore Island

[10] A Proton Transfer Reaction-Mass Spectrometer (PTR-MS) from Ionicon Analytik has been used for fast response measurements of oxygenated volatile organic compounds (OVOCs), NMHCs, acetonitrile and dimethyl sulfide ( $CH_3SCH_3$ ) at the University of New Hampshire's Thompson Farm Observing Station since July 2003 [*Talbot et al.*, 2005]. A second PTR-MS was deployed at Appledore Island for VOC measurements from 1 July to 13 August 2004, during the ICARTT summer campaign. Both instruments were run with a drift tube pressure of 2 mbar and an electric field of 600V while continuously stepping through a series of 30 masses. Of the 30 masses monitored, 6 masses

**Table 1.** Lifetime, Major Sources, and Removal Processes of Selected VOCs

Compound	$K_{OH} \times 10^{-12}$ $\text{cm}^3 \text{ molecule}^{-1} \text{ s}^{-1}$	$\tau_{OH}$ , <sup>a</sup> days	Removal Factor	Significance <sup>b</sup>	Reference <sup>c</sup>
CO	0.13	267	OH	U	1
C <sub>2</sub> H <sub>6</sub>	0.254	137	OH	U	1
C <sub>2</sub> H <sub>4</sub>	8.52	4.1	OH	U	1
C <sub>2</sub> H <sub>2</sub>	0.9	37	OH	U	3
C <sub>3</sub> H <sub>8</sub>	1.12	31	OH	U	1
C <sub>3</sub> H <sub>6</sub>	26.3	1.3	OH	U	1
i-butane	2.19	16	OH	U	2
n-butane	2.44	14	OH	U	1
i-C <sub>5</sub> H <sub>12</sub>	3.7	9.4	OH	U	2
n-C <sub>5</sub> H <sub>12</sub>	4	8.7	OH	U	2
C <sub>5</sub> H <sub>8</sub>	101	0.3	OH	Bi	2
C <sub>6</sub> H <sub>6</sub>	1.23	28	OH	U, A	3
C <sub>7</sub> H <sub>8</sub>	5.96	5.8	OH	U, A	3
C <sub>2</sub> Cl <sub>4</sub>	0.17	204	OH	U	4
CH <sub>2</sub> Br <sub>2</sub>	0.12	289	OH	Oc	4
CHBr <sub>3</sub>	0.15	232	OH, photolysis	Oc	4
CH <sub>2</sub> ClI	-	0.08	photolysis	Oc	4
2-PrONO <sub>2</sub>	0.29	120	OH	O	1
1-PrONO <sub>2</sub>	0.6	58	OH	O	1
2-BuONO <sub>2</sub>	0.92	38	OH	O	1
3-PenONO <sub>2</sub>	1.12	31	OH	O	3
2-PenONO <sub>2</sub>	1.85	19	OH	O	3
$\alpha$ -pinene	53.7	0.6	OH	Bi, A	2
$\beta$ -pinene	78.9	0.4	OH	Bi, A	2
Camphene	53	0.7	OH	Bi, A	2
Limonene	171	0.2	OH	Bi, A	2
CH <sub>3</sub> OH	0.944	37	OH	U, B, Bi	1
CH <sub>3</sub> COCH <sub>3</sub>	0.219	159	OH, photolysis	R, U, B, Bi	1
CH <sub>3</sub> SCH <sub>3</sub>	5	6.9	OH	Oc, A	1

<sup>a</sup>For  $[OH] = 3 \times 10^6 \text{ molecule cm}^{-3}$ .

<sup>b</sup>R, radical cycling; A, aerosol formation/modification; U, urban burning tracer; O, oxidation/processing indicator; Bi, biogenic emission tracer; Oc, ocean emission; B, biomass burning tracer.

<sup>c</sup>References: 1, *Atkinson et al.* [2000]; 2, *Atkinson* [1997]; 3, *Atkinson* [1990]; 4, *Sander et al.* [2006].

were used for diagnostic purposes while the other 24 masses corresponded to the VOCs of interest. The dwell time for each of the 24 masses was 20 s during the ICARTT campaign, yielding a total measurement cycle of  $\sim 10$  min. The systems were zeroed every 2.5 hours for 4 cycles by passing the flow through a catalytic converter (0.5% Pd on alumina at 450°C) to determine system background signals.

[11] Calibrations for the PTR-MS systems were conducted using three different high-pressure cylinders containing synthetic blends of selected NMHCs and OVOCs at the part per billion by volume (ppbv) level (Apel-Reimer Environmental, Inc.). Each of the cylinders used in the calibrations has an absolute accuracy of  $< \pm 5\%$  for all gases in each mix. Using volume dilution methods similar to those described by *Apel et al.* [1998], the standards were diluted to atmospheric mixing ratios (ppbv to pptv levels) with whole air passed through the catalytic converter to scrub all VOCs and maintain the same humidity as the air being sampled. The calibrations were conducted regularly on both instruments to monitor their performance and to quantify the mixing ratios of target gases. Additionally, mixing ratios for each gas were calculated by using the normalized counts per second which were obtained by subtracting out the nonzero background signal for each compound.

### 2.3. Methodology

[12] In this study, PCA was performed on chemical data obtained at AI and TF during ICARTT. This technique has

proved to be a robust method suitable for analyzing large atmospheric data sets [*Buhr et al.*, 1995, 1996; *Choi et al.*, 2003; *Wang et al.*, 2003]. In their aerosol particle characteristics study, *Saucy et al.* [1991] used PCA to examine compositions and time-dependent concentrations of aerosol particles collected near Phoenix, Arizona. They found three major sources for the majority of the particle types observed. *Swietlicki et al.* [1996] applied PCA to study urban air pollutants in Lund, a small city in southern Scandinavia with light industry. They found that the long-range transported air pollutants make up a significant part of the fine fraction aerosol. The sources related to traffic were mainly local in character while the rest constituted a regional background. These studies illustrate how PCA may facilitate source attribution of various pollutants. In this study, the representative characteristics of air masses were defined through PCA based on the variability of unique tracers, which then allowed identification of the major sources impacting air quality in the region.

[13] Typical chemical species representing various sources were chosen as tracers for this study. The major emission sources, removal processes, and photochemical lifetimes of selected species are provided in Table 1. This information is useful for identifying the origin and estimating the photochemical age of an air mass. Carbon monoxide (CO), several light alkanes and alkenes, and aromatics were chosen for their common source from combustion. Chloriodomethane (CH<sub>2</sub>ClI), dibromomethane (CH<sub>2</sub>Br<sub>2</sub>), bromoform (CHBr<sub>3</sub>), carbonyl sulfide (OCS), methyl chloride

(CH<sub>3</sub>Cl), methyl bromide (CH<sub>3</sub>Br), and CH<sub>3</sub>SCH<sub>3</sub> represent marine derived compounds [Zhou *et al.*, 2005]. Methylene chloride (CH<sub>2</sub>Cl<sub>2</sub>) and perchloroethylene (C<sub>2</sub>Cl<sub>4</sub>) are industrial solvents that have purely anthropogenic sources [Choi *et al.*, 2003]. The C<sub>1</sub>-C<sub>5</sub> alkyl nitrates are present as secondary photochemical products of parent hydrocarbons in photochemically aged air masses. Methanol (CH<sub>3</sub>OH) and acetone (CH<sub>3</sub>COCH<sub>3</sub>) have biogenic, oceanic and anthropogenic sources, with vegetative emissions being the largest at midlatitudes [Mao *et al.*, 2006; Jacob *et al.*, 2005; Singh *et al.*, 1994]. At TF, we also included four monoterpene species,  $\alpha$ -pinene,  $\beta$ -pinene, camphene, and limonene as additional indicators of biogenic sources. Propene (C<sub>3</sub>H<sub>6</sub>) and ethene (C<sub>2</sub>H<sub>4</sub>) are largely tracers of combustion with relatively short lifetimes (0.6–2.2 days) under a summertime OH concentration of  $\sim 1 \times 10^6$  molecules cm<sup>-3</sup>. High levels of these compounds indicate relatively fresh emissions from nearby sources. Toluene (C<sub>7</sub>H<sub>8</sub>, 3.6 days), benzene (C<sub>6</sub>H<sub>6</sub>, 19.3 days), ethyne (C<sub>2</sub>H<sub>2</sub>, 6.8 days), i-pentane (C<sub>5</sub>H<sub>10</sub>, 7.5 days), n-pentane (C<sub>5</sub>H<sub>12</sub>, 6.2 days), and n-butane (C<sub>4</sub>H<sub>10</sub>, 8.6 days) are also combustion-related tracers but have longer lifetimes. Benzene is a very good marker for automobile exhaust [Buhr *et al.*, 1996]. In contrast, the alkyl nitrates, e.g., 2-propyl nitrate (2-PrONO<sub>2</sub>), 1-propyl nitrate (1-PrONO<sub>2</sub>), 2-butyl nitrate (2-BuONO<sub>2</sub>), and 3-pentyl nitrate (3-PenONO<sub>2</sub>), have lifetimes > 1 week, and consequently their abundance indicates aged air masses potentially transported over long distances.

[14] During the entire ICARTT study period, there were 333 and 305 coincident observations of the 29 selected variables at AI and TF respectively. The data were z-scored and log transformed prior to analysis to ensure that all variables were weighted equally. Standard varimax eigenvector rotation was performed to generate an optimized distribution spread across the factor matrix, while the key eigen properties remained unaffected. Eigenvalues and factor loadings were computed, and the leading factors (i.e., air mass types) and relevant species identified by the largest factor loadings. The temporal variability of each factor score at AI and TF was examined to determine the dominant air mass types and concomitant time periods during ICARTT.

[15] To identify the major circulation patterns during ICARTT associated with the variability of pollutant mixing ratios in the dominant air mass types, the EOF approach [Wilks, 1995] was applied to sea level pressure (SLP). The National Centers for Environmental Prediction (NCEP) Global Final Analysis (FNL) <http://dss.ucar.edu/datasets/ds083.2> 6-hourly SLP data covering the eastern United States were used for the circulation pattern and EOF analyses. SLP was normalized by subtracting the seasonal mean SLP from each single SLP and then dividing by the standard deviation. The EOFs were determined on the correlation matrix of normalized SLP. The leading component represents the most frequent pattern that explains the largest variability in the data set, while subsequent components were determined with the constraint of orthogonality to the precedent ones. The resultant spatial patterns and score matrix were examined to pinpoint their relationships with the dominant air mass types. The eastern United States was selected as the analysis area to acquire a “big picture”

for the synoptic systems affecting New England. In addition, 4-day back trajectories were calculated using the Hybrid Single-Particle Lagrangian Integrated Trajectory (HY-SPLIT) model [Draxler and Hess, 1998] to locate source regions of different air mass types.

### 3. General Characteristics of the Key Compounds

[16] Time series of the mixing ratios of CO, C<sub>2</sub>H<sub>4</sub>, propane (C<sub>3</sub>H<sub>8</sub>), C<sub>7</sub>H<sub>8</sub>, CHBr<sub>3</sub>, and 2-ProNO<sub>2</sub> at AI and TF are presented in Figure 2. Ethene, C<sub>3</sub>H<sub>6</sub>, C<sub>3</sub>H<sub>8</sub>, C<sub>6</sub>H<sub>6</sub>, C<sub>7</sub>H<sub>8</sub>, and CO tracked each other well; their high levels clearly defined the occurrence of pollution episodes at both locations. In contrast, the temporal trends in alkyl nitrate species exhibited fewer periods of enhanced mixing ratios, but their highest concentrations did coincide with peaks in C<sub>2</sub>H<sub>4</sub>, C<sub>3</sub>H<sub>8</sub>, and C<sub>7</sub>H<sub>8</sub>. It should be noted that C<sub>3</sub>H<sub>8</sub> and C<sub>7</sub>H<sub>8</sub> had higher levels on AI than at TF, which might be due to slightly different source influences combined with a lower boundary layer height on AI than at TF. As expected, the time series of the marine tracers CHBr<sub>3</sub> and CH<sub>2</sub>Br<sub>2</sub> had similar variability and they were present in higher mixing ratios at AI compared to TF.

[17] Figure 3 showed the time series of isoprene (C<sub>5</sub>H<sub>8</sub>), CH<sub>3</sub>OH, CH<sub>3</sub>COCH<sub>3</sub> and monoterpenes measured at TF. During the whole campaign period CH<sub>3</sub>OH mixing ratios were larger than that of CH<sub>3</sub>COCH<sub>3</sub> and C<sub>5</sub>H<sub>8</sub>, but their temporal variability was quite similar. The diurnal cycles of  $\alpha$ -pinene and  $\beta$ -pinene had large daily amplitudes, and their time series showed similar characteristics that were out of phase with those of C<sub>5</sub>H<sub>8</sub>, CH<sub>3</sub>OH, and CH<sub>3</sub>COCH<sub>3</sub>.

[18] Hourly averaged diurnal cycles of several key biogenic and anthropogenic tracers are shown at TF and AI in Figure 4. At TF, C<sub>2</sub>H<sub>4</sub>, C<sub>3</sub>H<sub>6</sub>, C<sub>7</sub>H<sub>8</sub>, C<sub>6</sub>H<sub>6</sub>, and the four monoterpenes showed pronounced diurnal cycles with peaks mixing ratios occurring at night. The nighttime enhancements at TF result from the stable nocturnal inversion layer that effectively caps the emitted trace gases from the surface leading to their buildup at night with minimal loss via oxidation reactions [Talbot *et al.*, 2005]. In contrast, isoprene, CH<sub>3</sub>OH and CH<sub>3</sub>COCH<sub>3</sub> peaked during the day because of their biogenic origin whose source strength is dependent on temperature and solar radiation [Mao *et al.*, 2006]. At AI, C<sub>2</sub>H<sub>4</sub>, C<sub>3</sub>H<sub>6</sub>, C<sub>7</sub>H<sub>8</sub>, and C<sub>6</sub>H<sub>6</sub> showed similar diurnal cycles to those at TF but with smaller amplitudes, while mixing ratios of C<sub>5</sub>H<sub>8</sub>, CH<sub>3</sub>OH and CH<sub>3</sub>COCH<sub>3</sub> were somewhat flat throughout the day because of a stable marine boundary layer height and reduced biogenic sources.

## 4. Factor Loading and Air Mass Classification

### 4.1. Appledore Island

[19] The PCA suggests that at AI, the three most important factors (hereinafter termed as factors 1, 2, and 3) explained 82% of the total variance of the 29 species (Table 2). Factor 1 represented a combustion signature, as evidenced in the high factor loading (0.8–0.97) of C<sub>2</sub>H<sub>4</sub>, C<sub>3</sub>H<sub>6</sub>, C<sub>7</sub>H<sub>8</sub>, C<sub>6</sub>H<sub>6</sub>, C<sub>2</sub>H<sub>2</sub>, C<sub>5</sub>H<sub>10</sub>, C<sub>5</sub>H<sub>12</sub>, and C<sub>4</sub>H<sub>10</sub>. The high loading of the short-lived species C<sub>3</sub>H<sub>6</sub> and C<sub>2</sub>H<sub>4</sub> indicate relatively fresh emissions from a nearby urban area such as Portsmouth, New Hampshire (15 km), or highways (Interstate 95), or ships/boats in the Gulf of Maine. Iso-

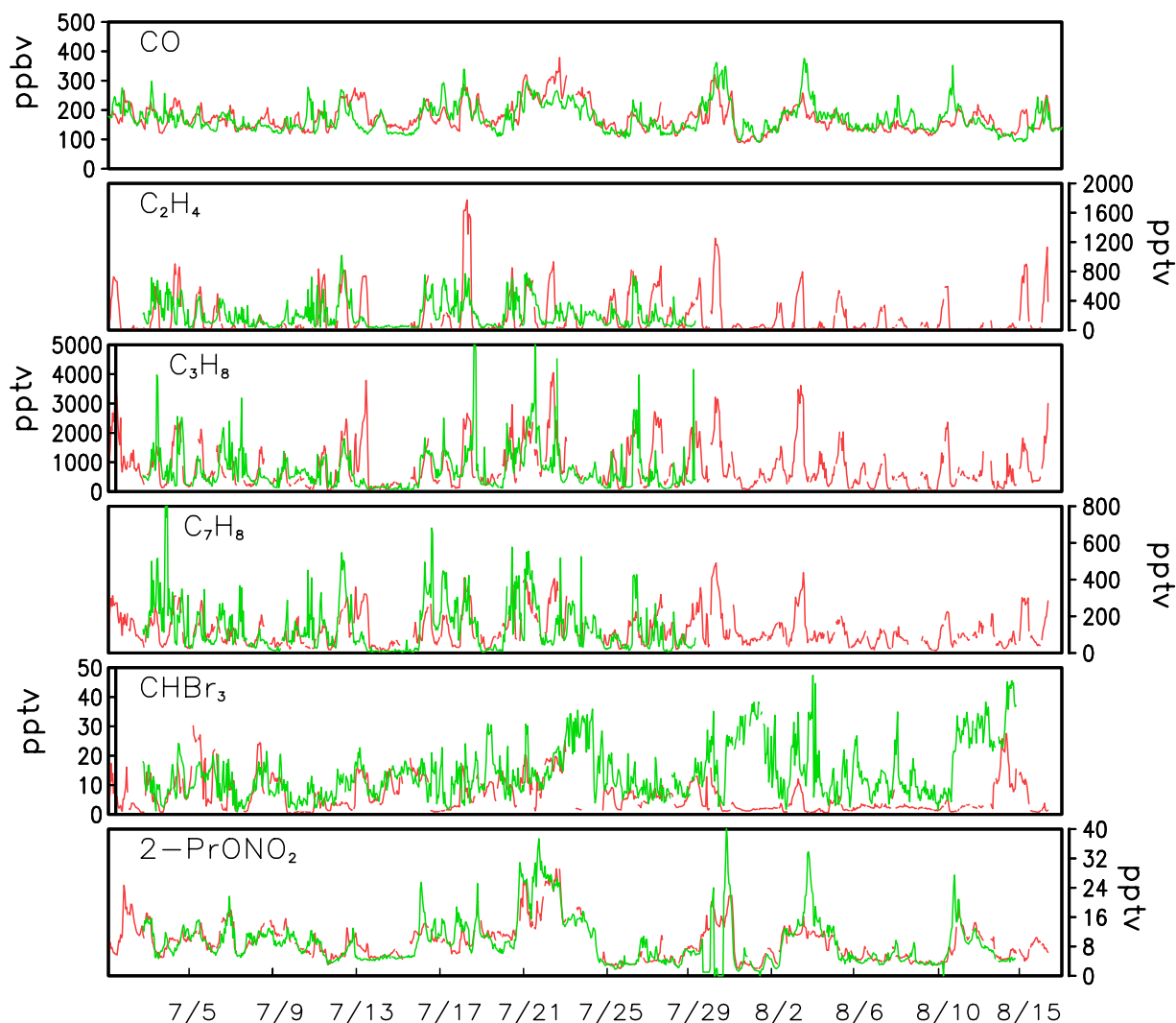


**Figure 2.** Time series of selected trace gases from AIRMAP measurements at TF (red) and AI (green).

prene,  $\text{CH}_3\text{OH}$  and  $\text{CH}_3\text{COCH}_3$  were also highly loaded (0.60–0.75) in this factor, indicating a terrestrial biogenic influence in continental outflow that reached AI. The moderate factor loadings of  $\text{CH}_2\text{Cl}_2$  and  $\text{C}_2\text{Cl}_4$  (0.4–0.5) suggests the presence of pollutants of industrial origin.

[20] The factor 2 loading was dominated by alkyl nitrates (0.82–0.95) and industrial solvents ( $\text{CH}_2\text{Cl}_2$ ,  $\text{C}_2\text{Cl}_4$ ) (0.75–0.77).  $\text{CH}_3\text{Cl}$  and  $\text{CH}_3\text{Br}$  also had factor loadings of 0.6–0.7, which implied that these photochemically aged air masses were influenced by terrestrial sources and/or anthro-

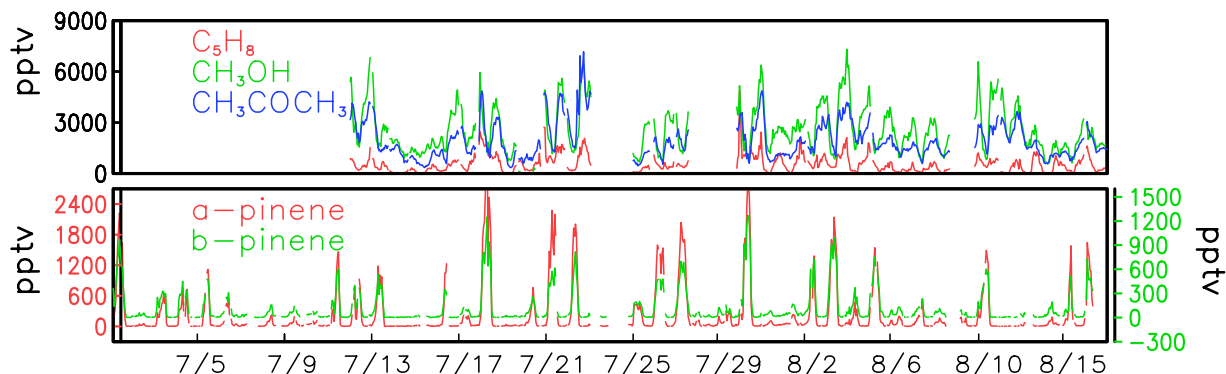


**Figure 3.** (top) Time series of  $\text{C}_5\text{H}_8$  (red),  $\text{CH}_3\text{OH}$  (green), and  $\text{CH}_3\text{COCH}_3$  (blue) and (bottom)  $\alpha$ -pinene (red),  $\beta$ -pinene (green) at Thompson Farm during ICARTT 2004.

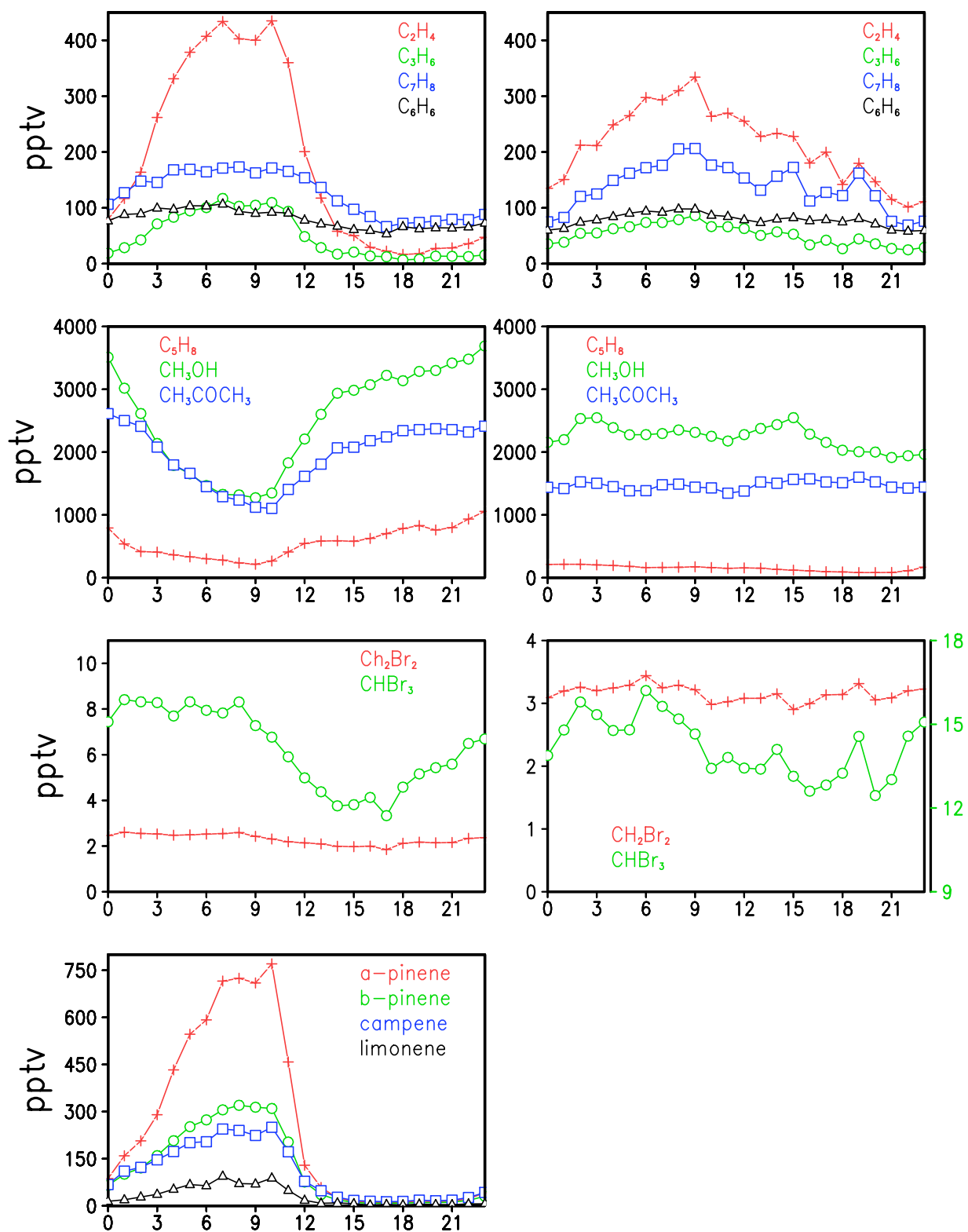


**Figure 4.** Observed diurnal cycle of biogenic and anthropogenic species at (left) TF and (right) AI.

pogenic inputs of these relatively long lived halocarbons. Our analysis cannot distinguish if these two species originated primarily from the ocean or urban pollution. Meteorological analysis was used (section 5) to facilitate our understanding of such issues.

[21] Factor 3 was heavily loaded with  $\text{CHBr}_3$ ,  $\text{CH}_2\text{Br}_2$ ,  $\text{CH}_3\text{SCH}_3$ , and  $\text{OCS}$ , suggesting air masses of oceanic origin. The fact that factor 3 was strongly anticorrelated with  $\text{CH}_3\text{OH}$  and  $\text{CH}_3\text{COCH}_3$  suggests that the ocean may be a sink of these two compounds, which is in agreement with the

**Table 2.** Factor Loadings for AI

Compound	Factor 1	Factor 2	Factor 3
CO	0.667	0.577	0.001
C <sub>2</sub> H <sub>6</sub>	0.640	0.537	0.084
C <sub>2</sub> H <sub>4</sub>	0.968	0.133	-0.082
C <sub>2</sub> H <sub>2</sub>	0.806	0.476	-0.011
C <sub>3</sub> H <sub>8</sub>	0.773	0.469	-0.123
C <sub>3</sub> H <sub>6</sub>	0.942	-0.078	0.005
i-butane	0.782	0.529	-0.158
n-butane	0.803	0.475	-0.194
C <sub>5</sub> H <sub>8</sub>	0.751	0.227	-0.083
C <sub>6</sub> H <sub>6</sub>	0.835	0.444	0.028
C <sub>7</sub> H <sub>8</sub>	0.898	0.279	-0.212
OCS	-0.409	0.238	0.637
CH <sub>3</sub> Cl	0.262	0.607	0.208
CH <sub>3</sub> Br	0.327	0.717	0.041
CH <sub>2</sub> Cl <sub>2</sub>	0.467	0.746	-0.009
C <sub>2</sub> Cl <sub>4</sub>	0.565	0.766	-0.099
CH <sub>2</sub> Br <sub>2</sub>	0.089	0.112	0.920
CHBr <sub>3</sub>	0.140	0.102	0.880
CH <sub>2</sub> ClI	-0.192	-0.256	0.784
2-PrONO <sub>2</sub>	0.210	0.952	0.040
1-PrONO <sub>2</sub>	0.099	0.931	0.165
2-BuONO <sub>2</sub>	0.226	0.933	0.044
3-PenONO <sub>2</sub>	0.305	0.883	-0.147
2-PenONO <sub>2</sub>	0.385	0.827	-0.220
C <sub>5</sub> H <sub>10</sub>	0.834	0.391	-0.237
C <sub>5</sub> H <sub>12</sub>	0.866	0.353	-0.223
CH <sub>3</sub> OH	0.629	0.107	-0.623
CH <sub>3</sub> COCH <sub>3</sub>	0.634	0.477	-0.479
CH <sub>3</sub> SCH <sub>3</sub>	-0.329	-0.216	0.716
Variance	58%	15%	9%

results from a regional budget study for the northeast United States by *Mao et al.* [2006] and *Marandino et al.* [2005] over the Pacific.

#### 4.2. Thompson Farm

[22] Four factors were extracted from the data matrix at TF and they accounted for 86% of the variance present in the original data set (Table 3). The first factor was a mixture of both biogenic and anthropogenic signatures with loading values of  $\sim 0.90$  for monoterpenes and  $0.71\text{--}0.95$  for light alkanes and alkenes. This indicates that factor 1 was a combination of combustion and biogenic emissions. The second factor was governed by alkyl nitrates, similar to factor 2 at AI. In factor 3, the predominance of biogenic emissions was indicated by high loadings of C<sub>5</sub>H<sub>8</sub>, CH<sub>3</sub>OH and CH<sub>3</sub>COCH<sub>3</sub>. Factors 1 and 3 together explained 64% of the total variance. The marine tracers CH<sub>2</sub>Br<sub>2</sub>, CHBr<sub>3</sub>, and CH<sub>3</sub>SCH<sub>3</sub> formed an anticorrelated suite in factor 3, suggesting that they may have loaded to another factor. This was confirmed in factor 4, which was heavily loaded with CH<sub>2</sub>Br<sub>2</sub>, CHBr<sub>3</sub>, and CH<sub>2</sub>ClI.

#### 4.3. Air Mass Classification and Their Temporal Variability

[23] On the basis of the results from sections 4.1 and 4.2, air mass types were assigned according to the species photochemical lifetimes in those major factors. For both AI and TF, factor 1 was highly loaded with relatively short lived emissions from combustion, including mobile sources. Thus the air mass type for factor 1 is referred to as a recent anthropogenic air mass, despite the fact that for TF it was also loaded with highly reactive monoterpenes. The high loadings of monoterpenes for factor 1 at TF are quite

understandable considering the fact that monoterpenes and NMHCs have quite similar diurnal cycles, whereas C<sub>5</sub>H<sub>8</sub>, CH<sub>3</sub>OH and CH<sub>3</sub>COCH<sub>3</sub> are out of phase with them (Figure 4). Thus the PCA results show that similar variability in the occurrence of compounds does not necessarily assure that they have a common source.

[24] Factor 2 was heavily loaded with long-lived alkyl nitrates and anthropogenic tracers indicative of photochemically aged and processed air masses. Such air masses traveled over a long distance probably originating from the mid-Atlantic and Midwest urban/industrial areas [*Mao and Talbot*, 2004]. To further locate their major source regions, we simulated 96-hour back trajectories during days when factors 1 and 2 were prevalent at AI. Indeed we found that for factor 1, air mass mainly came from over land in the proximity of AI (Figure 5a), whereas for factor 2 the air mass mainly came from the northeast urban corridor and occasionally the Ohio Valley (Figure 5b). Thus factor 2 was referred to as an aged/processed anthropogenic air mass of urban-industrial origin. Factor 3 for AI and factor 4 for TF represented air mass from the marine boundary layer and thus were referred to as a recent marine biogenic air mass. Factor 3 at TF is referred to as a terrestrial biogenic air mass, as it bears significant loadings for C<sub>5</sub>H<sub>8</sub>, CH<sub>3</sub>OH, and CH<sub>3</sub>COCH<sub>3</sub>, which have abundant biogenic sources [*Guenther et al.*, 1995; *Mao et al.*, 2006].

[25] The factor score of each principal component at AI and TF is shown as a function of time in Figure 6. The time series of factor scores illustrate the temporal variability in the occurrence of various air masses at each site. Comparing information in Figure 6 with that in Figures 2 and 3, we found that the peak score values of factor 1 at AI (TF) clearly corresponded to high levels of C<sub>2</sub>H<sub>4</sub> at AI (TF), while those

**Table 3.** Factor Loadings for TF

Compound	Factor 1	Factor 2	Factor 3	Factor 4
CO	0.651	0.667	0.173	0.179
C <sub>2</sub> H <sub>6</sub>	0.502	0.735	0.098	0.042
C <sub>2</sub> H <sub>4</sub>	0.953	0.082	-0.121	0.095
C <sub>2</sub> H <sub>2</sub>	0.718	0.551	0.182	0.193
C <sub>3</sub> H <sub>8</sub>	0.874	0.304	-0.067	0.106
C <sub>3</sub> H <sub>6</sub>	0.940	0.047	-0.133	0.071
i-butane	0.828	0.456	0.089	0.133
n-butane	0.795	0.518	0.164	0.067
C <sub>5</sub> H <sub>8</sub>	0.155	0.213	0.758	-0.149
C <sub>6</sub> H <sub>6</sub>	0.759	0.517	0.116	0.095
C <sub>7</sub> H <sub>8</sub>	0.815	0.370	0.065	0.125
C <sub>2</sub> Cl <sub>4</sub>	0.484	0.728	0.059	0.216
CH <sub>2</sub> Br <sub>2</sub>	0.291	0.293	-0.131	0.839
CHBr <sub>3</sub>	0.515	0.196	-0.169	0.741
CH <sub>2</sub> ClI	-0.281	-0.178	0.012	0.824
2-PrONO <sub>2</sub>	0.179	0.939	0.134	0.106
1-PrONO <sub>2</sub>	0.170	0.952	0.160	0.060
2-BuONO <sub>2</sub>	0.119	0.970	0.076	0.019
3-PenONO <sub>2</sub>	0.232	0.946	0.050	-0.010
2-PenONO <sub>2</sub>	0.159	0.947	0.074	-0.025
C <sub>5</sub> H <sub>10</sub>	0.845	0.408	0.172	0.116
C <sub>5</sub> H <sub>12</sub>	0.865	0.395	0.122	0.078
$\alpha$ -pinene	0.926	0.043	-0.145	-0.037
$\beta$ -pinene	0.893	0.046	-0.135	-0.033
Camphene	0.907	0.227	-0.039	-0.018
Limonene	0.894	0.086	-0.074	0.008
CH <sub>3</sub> OH	-0.357	0.146	0.856	-0.066
CH <sub>3</sub> COCH <sub>3</sub>	0.021	0.440	0.760	-0.070
CH <sub>3</sub> SCH <sub>3</sub>	-0.224	0.043	-0.436	0.028
Variance	56%	17%	8%	5%

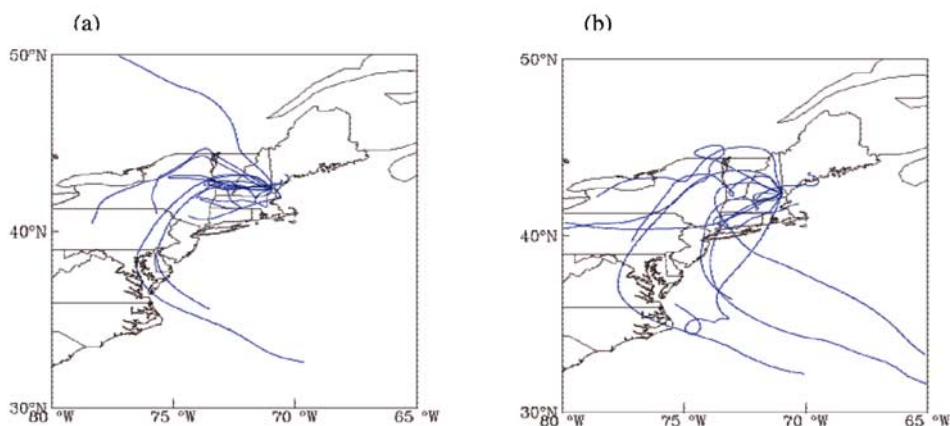


**Figure 5.** Backward air mass trajectories for representative days dominant by (a) factor 1 and (b) factor 2 at AI.

of factor 2 corresponded to high level of 2-PrONO<sub>2</sub> at both sites. Factor score for the third component at TF was highly and positively correlated with the mixing ratios of biogenic tracers C<sub>5</sub>H<sub>8</sub>, CH<sub>3</sub>OH and CH<sub>3</sub>COCH<sub>3</sub>. Differences between

factor scores, therefore, can be used to identify the dominant air mass type at a specific time. A given time period with a dominance of one specific factor, and hence its corresponding air mass type, was selected when the factor score was equal

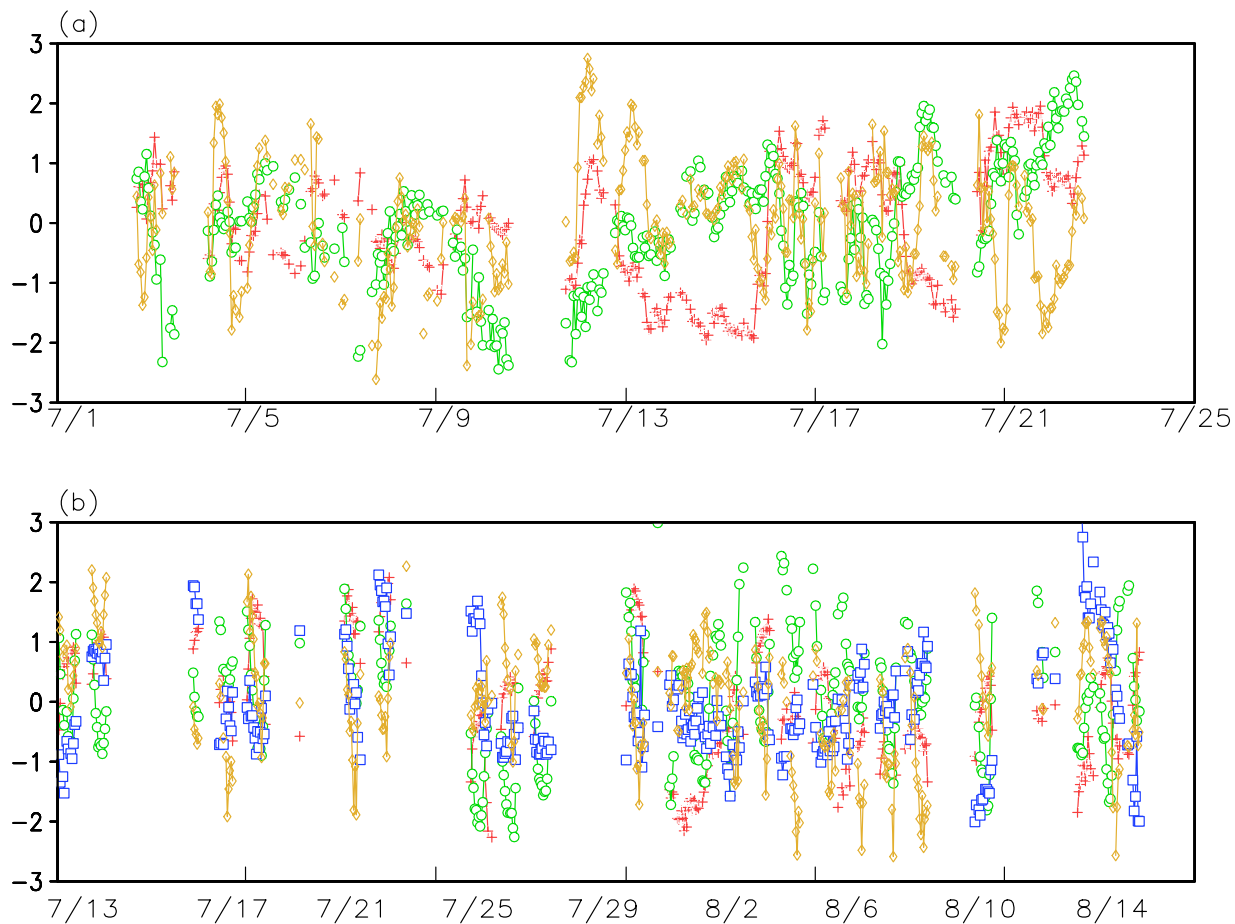


**Figure 6.** Time series of factor scores of the principal components extracted in the PCA for observations at (a) AI (red for factor 1, green for factor 2, and yellow for factor 3) and (b) TF (red for factor 1, green for factor 2, blue for factor 3, and yellow for factor 4). The time periods correspond to intervals when the selected species occurred coincidentally during ICARTT.

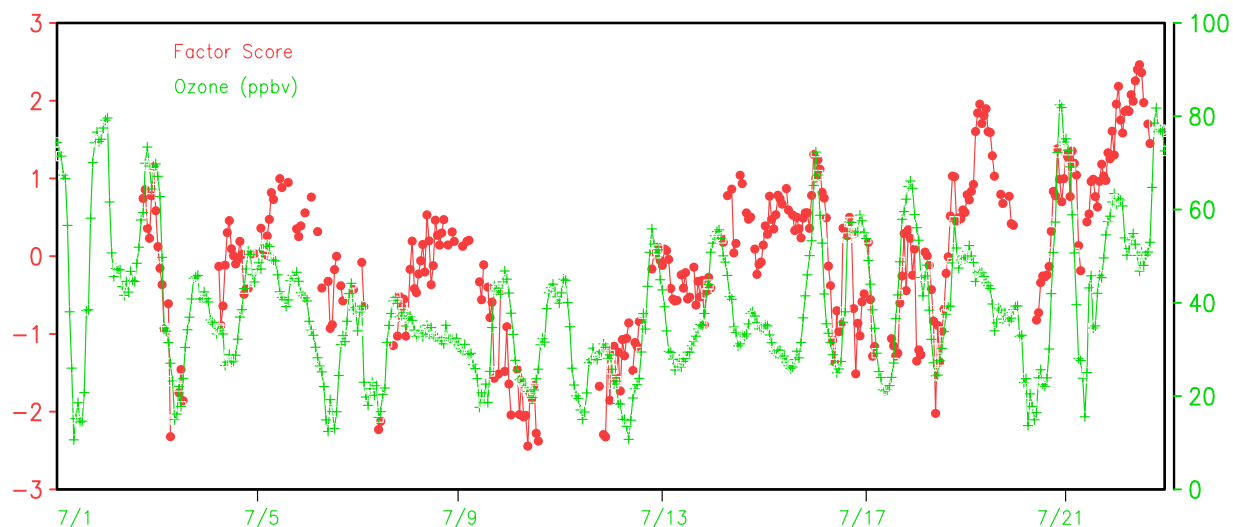


**Figure 7.** Time series of  $O_3$  mixing ratios and factor 2 (aged/processed air mass of urban-industrial origin) score at AI.

to or greater than one standard deviation. Circulation patterns at the selected time periods were examined to determine the association between meteorological conditions and the dominant air mass type.

[26] At AI, recent anthropogenic air mass and marine biogenic air mass each comprised 16% of the observational period, while aged/processed anthropogenic air mass of urban-industrial origin accounted for 14%. At TF, 19% of the period was governed by recent anthropogenic air mass, 17% by aged/processed air mass of urban-industrial origin, 15% by terrestrial biogenic air mass, and 14% by recent marine biogenic air mass. Overall, 46% of the campaign period at AI and 65% at TF was dominated by a specific air mass type. Over the remaining time period, ambient levels of pollutants were determined by a mixture of different air mass types.

[27] At both TF and AI, nearby emission sources made the largest contribution (58% on AI and 56% at TF) to the total variance (58% on AI and 56% at TF) of the data set, whereas long-distance transport contributed much less (15% on AI and 17% at TF). However, this does not necessarily mean that nearby sources were more important in ambient levels of trace gases than distant upwind sources. In fact, the contribution of nearby emission sources was not strong enough to trigger the occurrence of heavy pollution episodes during the ICARTT study period. However, when long-range transport did have a local impact, strong pollution events were more likely to occur. This feature is illustrated in Figure 7, which highlights the fact that higher  $O_3$  mixing ratios accompanied the aged/processed anthropogenic air mass influenced time periods. In addition, many of the large spikes in VOCs (Figure 2) were also associated with long-range transport.

[28] It is worth noting that 30% of the ICARTT time period on AI was dominated by recent and aged/processed anthropogenic air masses, which is only slightly smaller than that at TF (36%). Similarly, 14% of the time period at TF and 16% at AI was influenced by recent marine biogenic air masses. These two results clearly show the strong impact of continental outflow on the nearshore marine atmosphere,

and conversely an important impact of marine emissions at an inland site.

## 5. Relationship Between Circulation Patterns and Air Mass Types

### 5.1. Identification of Circulations for Each Air Mass Type

[29] The corresponding circulation pattern was identified for each time period when one specific air mass type was prevalent at TF or AI. Representative circulation patterns for the various air mass types are depicted in Figures 8a–8e, respectively. During the periods when recent anthropogenic air masses dominated, the Atlantic subtropical high was strong and covered the U.S. east coast from Florida to Maine (Figure 8a). This circulation pattern generates stagnant synoptic conditions in the northeast, leading to buildup of pollution influences from local emissions in a boundary layer with weak ventilation.

[30] Typical circulation patterns that facilitated long-distance transport into New England are presented in Figures 8b and 8c. In the first case a trough was positioned over the Great Lakes in tandem with the subtropical high over the western Atlantic (Figure 8b). In between, southwesterly flow transported air masses from densely populated and industrial areas of Pennsylvania, New Jersey, New York and the Great Boston area to southern New Hampshire. A second route was established when a strong low disturbance was centered along the U.S. east coast and extended northward over New England (Figure 8c). The cyclonic flow brought air masses originating from the mid-Atlantic and the southeast out over the Atlantic toward the northeast with subsequent landfall in coastal New Hampshire/Maine/Massachusetts [Mao and Talbot, 2004]. This transport scenario was evidenced by the high levels of ozone and alkyl nitrates in the air masses arriving at TF and AI.

[31] The final two circulation patterns shown in Figures 8d and 8e are from time periods when marine tracers were dominant at our study sites. Here a strong subtropical high prevailed over the western Atlantic, while a ridge extended

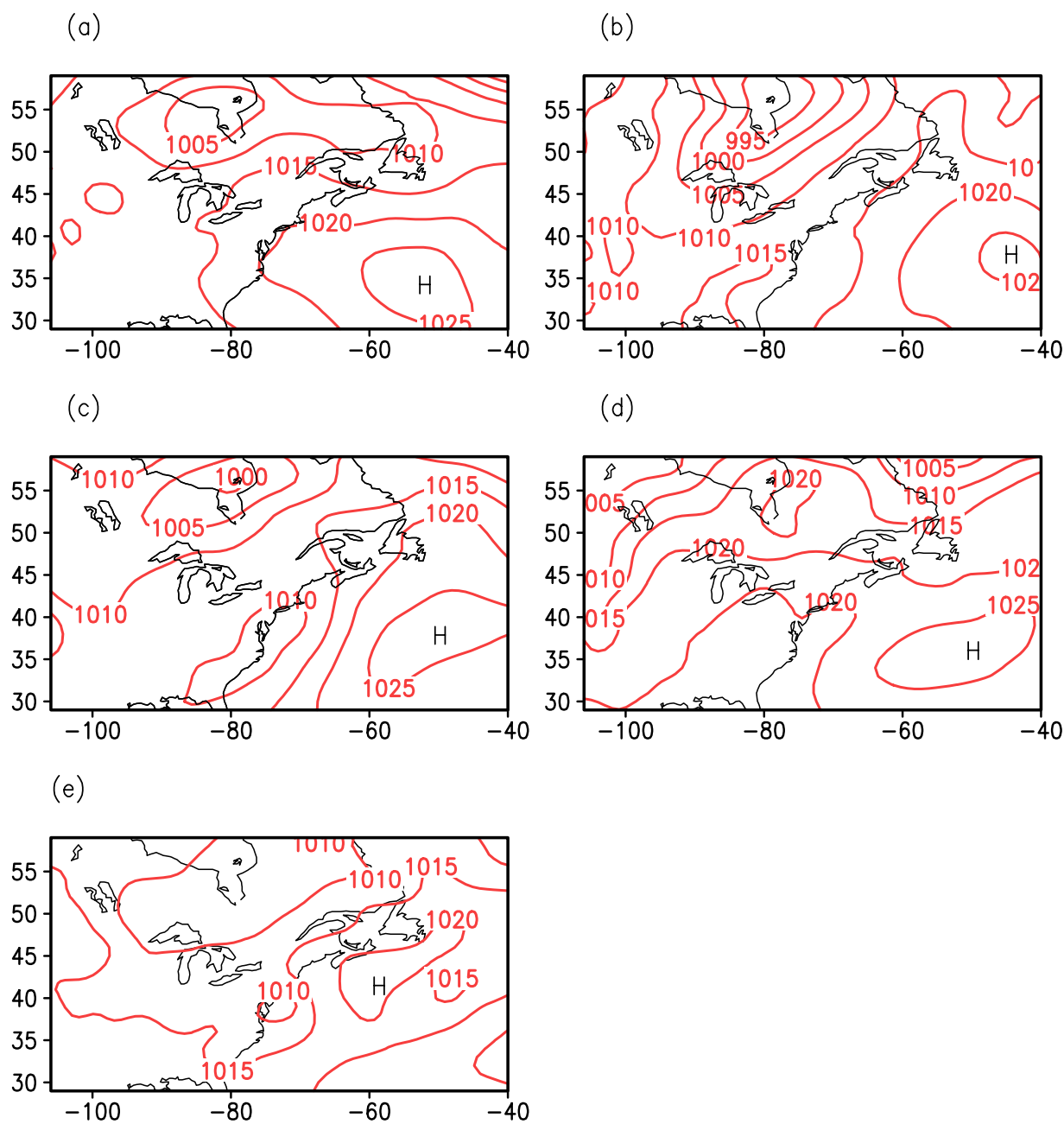


**Figure 8.** Typical circulation patterns corresponding to time periods when various air mass types were dominant: (a) recent anthropogenic air masses, (b and c) aged/processed anthropogenic air masses of urban-industrial origin, and (d and e) recent marine biogenic air masses.

from the southeastern United States to Connecticut (Figure 8d). Anticyclonic circulation brought air masses from the marine boundary layer to the New Hampshire coastal area, leading to large mixing ratios of marine tracers. Another circulation pattern occurred frequently during periods of elevated marine derived tracers. This happened when the subtropical high was strong and reached northward to the Maine and Canadian coasts. At the same time a weak low pressure disturbance centered in Maryland evolved into a trough along the east coast (Figure 8e). The southwesterly flow along the east edge of this low disturbance turned southeasterly and merged with flows from the western edge of the subtropical high to reach coastal New

Hampshire. Both flows originated from the Atlantic and resulted in high levels of marine tracers.

## 5.2. Circulations and Dominant Air Mass Types During Summer 2004

[32] The daily maximum level of  $O_3$  at TF during summer 2004 never exceeded 125 ppbv, and there were only 6 days with a daily maximum  $O_3 > 80$  ppbv. J. Hegarty et al. (Meteorological controls on summertime surface ozone in the northeastern United States, submitted to *Journal of Geophysical Research*, 2007) found that over the period of 2000–2004, summertime domain-averaged  $O_3$  across the northeast reached a minimum of 52 ppbv in 2004. This

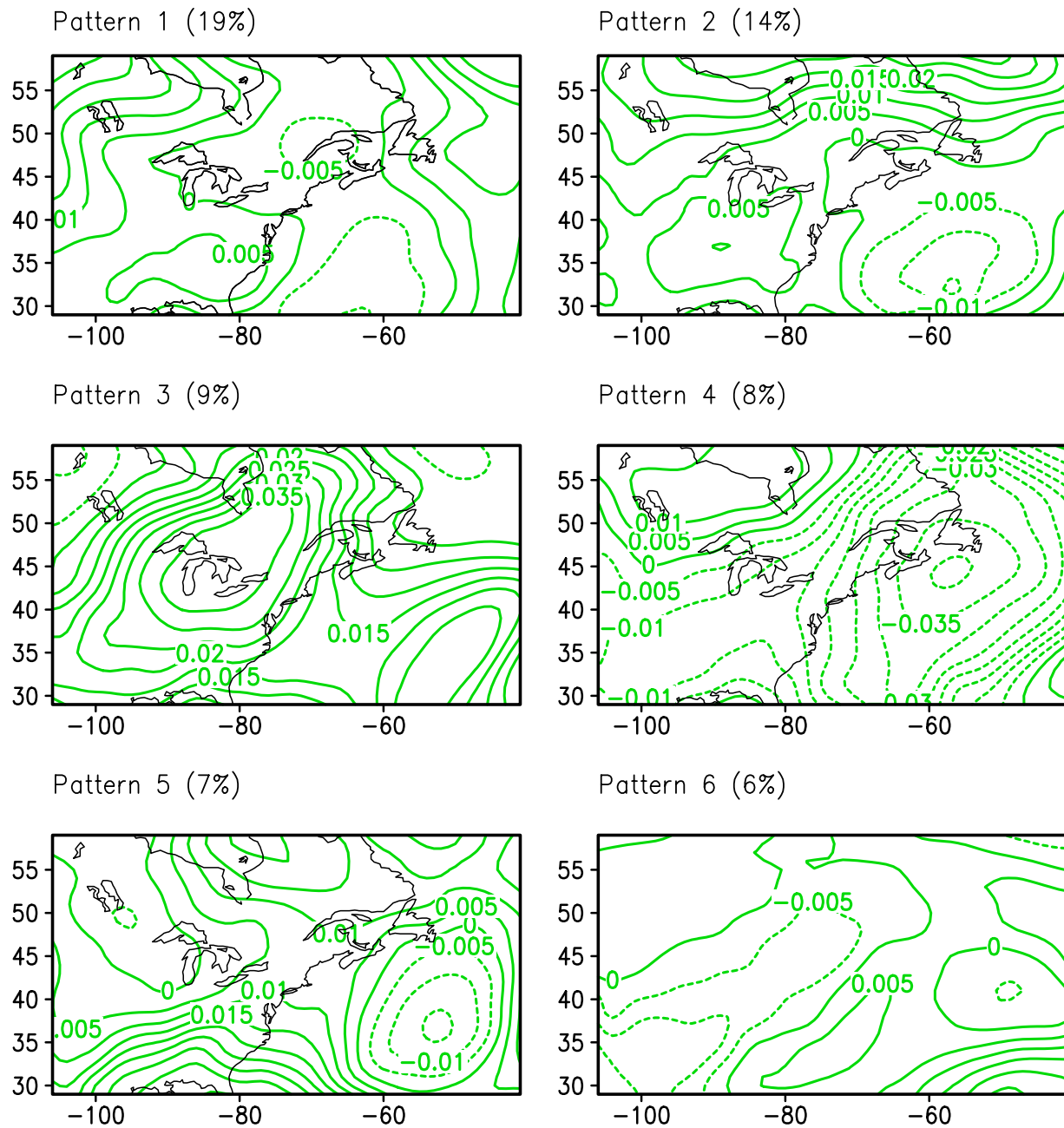


**Figure 9.** Spatial patterns corresponding to the six EOFs for summer 2004.

departed from the 5-year mean and was statistically significant at the 90% confidence level. Using  $O_3$  as an indicator of air quality, summer 2004 was relatively “cleaner” than the previous 4 years. As presented in section 4.3, air masses from long-range transport commonly trigger the occurrence of high  $O_3$  pollution episodes in New England. To understand whether dynamical processes were a factor in the fewer occurrences of  $O_3$  episodes in summer 2004, the predominant circulation patterns were identified using EOF analysis.

[33] The first six dominant circulation patterns obtained from the EOF analysis explained 63% of the variance for SLP over the ICARTT study period (Figure 9). Pattern 1 was a shallow trough moving through northern New England with the North Atlantic Subtropical High (NASH) centered east of 60°W and ~30°N. New Hampshire was

under the control of northwesterly flow from central Canada. In pattern 2, the NASH shifted to the northeast, with its center located west of 60°W, around 45°N. Coastal New Hampshire was under the influence of easterly south-easterly flow from the Atlantic. In pattern 3, a strong high-pressure system covered a large area of the western Atlantic and the eastern United States. The weather was calm with weak surface winds. Pattern 4 was similar to pattern 1, but the trough was much deeper and intruded southward to the mid-Atlantic area. Pattern 5 was characterized by a strong NASH in the southeastern United States with the ridge reaching the New England area. The ridge efficiently blocked flows from the urban-industrial areas of the mid-Atlantic states to New England. Pattern 6 showed a low trough extending southwest from the northeast United

**Table 4.** Correlations Between the Six EOF and Representative Patterns Dominant by Various Air Masses as Shown in Figures 8–10

	EOF					
	Pattern 1	Pattern 2	Pattern 3	Pattern 4	Pattern 5	Pattern 6
Figure 8a	−0.64	−0.81	0.61	−0.35	−0.36	0.08
Figure 8b	0.26	−0.09	−0.47	−0.04	−0.05	0.70
Figure 8c	−0.24	−0.28	0.03	−0.28	−0.10	0.60
Figure 8d	−0.52	−0.48	0.39	−0.24	0.05	0.33
Figure 8e	−0.55	−0.54	0.42	−0.23	0.13	0.20

States covering the whole Ohio valley, while NASH controlled the western Atlantic. This was the typical pattern that favored southwesterly flows from areas such as New Jersey and New York to New England.

[34] Compared to previous summers, the subtropical high was much weaker in summer 2004 while the low trough along the east coast was deeper. In addition, the high pressure over the eastern United States was stronger and often extended as far south as the Gulf coast. These characters in circulation patterns suggested cooler, drier, and relatively cleaner air from central Canada brought into the northeast in summer 2004 compared to previous years.

[35] The spatial correlation coefficients ( $r$ ) between these six patterns as revealed by EOF analysis and the circulation patterns from Figure 8 were calculated (Table 4). The strongest positive correlations were found between pattern 3 and the circulation from Figure 8a ( $r = 0.61$ ), and between pattern 6 and the circulation from Figures 8b and 8c ( $r = 0.7$  and  $0.6$  respectively). This indicates that under circulation pattern 3, air masses with high mixing ratios of pollutants from nearby sources were dominant in New Hampshire, while under circulation pattern 6 air masses with high loadings of alkyl nitrates from long-distance transport dominated. We propose that under influence of pattern 3 the high pressure system controlled the eastern United States resulting in clear weather and calm winds; under pattern 6, the strong pressure gradient between the low trough over the Ohio valley and the subtropical high over the western Atlantic facilitated transport of photochemically aged air from the northeast urban corridor to New Hampshire.

[36] Clearly, patterns 3 and 6 are two synoptic circulation patterns conducive to the occurrence of high levels of either recent or aged/processed anthropogenic VOCs along eastern New England. However, the fact that pattern 3 explained 9% and pattern 6 only 6% of the total variance in SLP implies that these two patterns were not the most representative circulation patterns for summer 2004. In contrast, the most important circulation pattern (pattern 1) was negatively correlated with those shown in Figure 8. As mentioned previously, pattern 1 indicates that the dominant synoptic circulation pattern during summer 2004 was a trough positioned over the northeast, leaving the coastal New England region often under the control of north-northwesterly flow from central Canada. This is likely the primary reason why summer 2004 was from an air quality standpoint, a “cleaner” than average year [White *et al.*, 2007].

## 6. Conclusions

[37] In this study PCA was conducted on chemical data collected at AI and TF during the summer 2004 ICARTT

campaign to identify the dominant air mass types, their sources, and temporal variability. The EOF approach was applied to SLP data to pinpoint the most representative circulation patterns and to explore the meteorological processes that contributed to the variability of dominant air masses.

[38] Three major findings emerged from this study. First, three dominant air mass types, i.e., recent anthropogenic, aged/processed of urban-industrial origin, and recent marine biogenic, were identified at TF and AI, and an extra terrestrial biogenic air mass type was also defined for TF. Second, nearby emission sources contributed most significantly to the total variance from the entire data set (58% on AI and 56% at TF), whereas the long-distance transport contributed much less (15% on AI and 17% at TF). However, when air masses were transported from long distances and reached New England, pollution events with high levels of  $O_3$  and other pollutants were likely to dominate. This indicates that air masses from distant sources appeared to be closely associated with the occurrence of pollution episodes in southern New Hampshire in spite of the fact that they only impacted the region periodically. Third, the EOF analysis revealed that the most important circulation pattern was characterized by a trough locating along coastal New England, leaving this area under control of northwesterly flow from central Canada. In contrast, the two major circulation patterns associated with dominance of recent and aged/processed anthropogenic air masses of urban/industrial origin were both less significant in summer 2004. Analysis of synoptic circulation in summer 2004, as compared to previous years 2001, 2002, and 2003, have showed that a weaker subtropical high and a deeper low trough along the east coast contributed to fewer high ozone episodes and a lower seasonal average ozone level. This may be the primary reason why regional air quality in summer 2004 was cleaner than in previous years. This result highlighted the importance of meteorological circulation patterns in determining the air quality in New England.

[39] The major differences between AI and TF was that the terrestrial biogenic emissions were a significant source of VOCs at TF, while at AI the biogenic signals were mixed into continental outflow and were less pronounced. This also reflected the loss of biogenic compounds through oxidation during transport from the continent to AI. It is also worth noting that at the marine site AI, recent and aged/processed anthropogenic air masses impacted air quality during 30% of the studying period while marine biogenic air masses only accounted for 16%. This is quite similar to the situation found at the inland site TF, where recent and aged/processed anthropogenic air masses dominated 36% of the time while marine biogenic air masses accounted for

14%. These results clearly show strong impacts of continental outflow on the nearshore marine atmosphere and likewise and influence from marine biogenic emissions inland.

[40] **Acknowledgments.** Financial support for this work was provided through the Office of Oceanic and Atmospheric Research at NOAA under grants NA04OAR4600154 and NA05OAR4601080 and the Environment Protection Agency under grant RD-83145401.

## References

- Apel, E. C., J. G. Calvert, J. P. Greenberg, D. Riemer, R. Zika, T. E. Kleindienst, W. A. Lonneman, K. Fung, and E. Fujita (1998), Generation and validation of oxygenated volatile organic carbon standards for the 1995 Southern Oxidants Study Nashville Intensive, *J. Geophys. Res.*, *103*, 22,281–22,294.
- Atkinson, R. (1990), Gas-phase tropospheric chemistry of organic compounds—A review, *Atmos. Environ.*, *24*, 1–41.
- Atkinson, R. (1997), Gas-phase tropospheric chemistry of volatile organic compounds: 1. Alkanes and alkenes, *J. Phys. Chem. Ref. Data*, *26*, 215–290.
- Atkinson, R., D. L. Baulch, R. A. Cox, R. F. Hampson, J. A. Kerr, M. J. Rossi, and J. Troe (2000), Evaluated kinetic and photochemical data for atmospheric chemistry: Supplement VIII, Halogen species—IUPAC Subcommittee on Gas Kinetic Data Evaluation for Atmospheric Chemistry, *J. Phys. Chem. Ref. Data*, *29*, 167–266.
- Buhr, M. P., et al. (1995), Evaluation of ozone precursor source type using principal component analysis of ambient air measurement in rural Alabama, *J. Geophys. Res.*, *100*(D11), 22,853–22,860.
- Buhr, M., D. Sueper, M. Trainer, P. Goldan, B. Kuster, F. Fehsenfeld, G. Kok, R. Shillawski, and A. Schanot (1996), Trace gas and aerosol measurements using aircraft data from the North Atlantic Regional Experiment (NARE 1993), *J. Geophys. Res.*, *101*(D22), 29,013–29,028.
- Choi, Y., S. Elliott, I. J. Simpson, D. R. Blake, J. J. Colman, M. K. Dubey, S. Meinardi, F. S. Rowland, T. Shirai, and F. A. Smith (2003), Survey of whole air data from the second airborne biomass burning and lightning experiment using principal component analysis, *J. Geophys. Res.*, *108*(D5), 4163, doi:10.1029/2002JD002841.
- Cooper, O. R., J. L. Moody, D. D. Parrish, M. Trainer, T. B. Ryerson, J. S. Holloway, G. Hubler, F. C. Fehsenfeld, S. J. Oltmans, and M. J. Evans (2001), Trace gas signatures of the airstreams within North Atlantic cyclones: Case studies from the North Atlantic Regional Experiment (NARE '97) aircraft intensive, *J. Geophys. Res.*, *106*(D6), 5437–5456.
- Draxler, R. R., and G. D. Hess (1998), An overview of HY-SPLIT 4 modeling system for trajectories, dispersion, and deposition, *Aust. Meteorol. Mag.*, *47*, 295–308.
- Goldan, P. D., W. C. Kuster, E. Williams, P. C. Murphy, F. C. Fehsenfeld, and J. Meagher (2004), Nonmethane hydrocarbon and oxy hydrocarbon measurements during the 2002 New England Air Quality Study, *J. Geophys. Res.*, *109*, D21309, doi:10.1029/2003JD004455.
- Griffin, R. J., C. A. Johnson, R. W. Talbot, H. Mao, R. S. Russo, Y. Zhou, and B. C. Sive (2004), Quantification of ozone formation metrics at Thompson Farm during the New England Air Quality Study (NEAQS) 2002, *J. Geophys. Res.*, *109*, D24302, doi:10.1029/2004JD005344.
- Guenther, A., et al. (1995), A global model of natural volatile organic compound emissions, *J. Geophys. Res.*, *100*(D5), 8873–8892.
- Jacob, D. J., B. D. Field, Q. Li, D. R. Blake, J. de Gouw, C. Warneke, A. Hansel, A. Wisthaler, H. B. Singh, and A. Guenther (2005), Global budget of methanol: Constraints from atmospheric observations, *J. Geophys. Res.*, *110*, D08303, doi:10.1029/2004JD005172.
- Mao, H., and R. Talbot (2004), Role of meteorological processes in two New England ozone episodes during summer 2001, *J. Geophys. Res.*, *109*, D20305, doi:10.1029/2004JD004850.
- Mao, H., R. Talbot, C. Nielsen, and B. Sive (2006), Controls on methanol and acetone in marine and continental atmospheres, *Geophys. Res. Lett.*, *33*, L02803, doi:10.1029/2005GL024810.
- Marandino, C. A., W. J. De Bruyn, S. D. Miller, M. J. Prather, and E. S. Saltzman (2005), Oceanic uptake and the global atmospheric acetone budget, *Geophys. Res. Lett.*, *32*, L15806, doi:10.1029/2005GL023285.
- Merrill, J. T., and J. L. Moody (1996), Synoptic meteorology and transport during the North Atlantic Regional Experiment (NARE) intensive: Overview, *J. Geophys. Res.*, *101*(D22), 28,903–28,921.
- Moody, J. L., II, G. L. Forbes, M. Trainer, and M. Buhr (1996), Meteorological mechanisms for transporting O<sub>3</sub> over the western North Atlantic Ocean: A case study for August 24–29, 1993, *J. Geophys. Res.*, *101*(D22), 29,213–29,228.
- Ray, J. D., R. L. Heaven, and M. Flores (1996), Surface level measurement of ozone and precursors at coastal and offshore locations in the Gulf of Maine, *J. Geophys. Res.*, *101*(D22), 29,005–29,011.
- Russo, R. S. (2005), Alkyl nitrate distributions at Thompson Farm and Appledore Island, paper presented at ICARTT 2005 Data Analysis Workshop, Earth Syst. Res. Lab., NOAA, Univ. of N. H., Durham, 9–12 Aug.
- Sander, S.P., et al. (2006), Chemical kinetics and photochemical data for use in atmospheric studies, evaluation 15, *JPL Publ.*, 06-2, NASA Jet Propul. Lab., Pasadena, Calif.
- Saucy, D. A., J. R. Anderson, and P. R. Buseck (1991), Aerosol particle characteristics determined by combined cluster and principal component analysis, *J. Geophys. Res.*, *96*(D4), 7403–7414.
- Seaman, N. L., and S. A. Michelson (2000), Mesoscale meteorological structure of a high-ozone episode during the 1995 NARSTO-Northeast study, *J. Appl. Meteorol.*, *39*, 384–398.
- Singh, H. B., D. O'Hara, D. Herlth, W. Sachse, D. R. Blake, J. D. Bradshaw, M. Kanakidou, and P. J. Crutzen (1994), Acetone in the atmosphere: Distribution, sources, and sinks, *J. Geophys. Res.*, *99*(D1), 1805–1820.
- Sive, B. C., Y. Zhou, D. Troop, Y. Wang, W. C. Little, O. W. Wingenter, R. S. Russo, R. K. Varner, and R. Talbot (2005), Development of a cryogen-free concentration system for measurements of volatile organic compounds, *Anal. Chem.*, *77*(21), 6989–6998, doi:10.1021/ac0506231.
- Swietlicki, E., S. Puri, H. C. Hansson, and H. Edner (1996), Urban air pollution source apportionment using a combination of aerosol and gas monitoring techniques, *Atmos. Environ.*, *30*(15), 2795–2809.
- Talbot, R., H. Mao, and B. Sive (2005), Diurnal characteristics of surface level O<sub>3</sub> and other important trace gases in New England, *J. Geophys. Res.*, *110*, D09307, doi:10.1029/2004JD005449.
- Wang, Y., et al. (2003), Intercontinental transport of pollution manifested in the variability and seasonal trend of springtime O<sub>3</sub> at northern middle and high latitudes, *J. Geophys. Res.*, *108*(D21), 4683, doi:10.1029/2003JD003592.
- White, A. B., L. S. Darby, C. J. Senff, C. W. King, R. M. Banta, J. Koerner, J. M. Wilczak, P. J. Neiman, W. M. Angevine, and R. Talbot (2007), Comparing the impact of meteorological variability on surface ozone during the NEAQS (2002) and ICARTT (2004) field campaigns, *J. Geophys. Res.*, *112*, D10S14, doi:10.1029/2006JD007590.
- Wilks, D. S. (1995), *Statistical Methods in the Atmospheric Sciences: An Introduction*, 467 pp., Elsevier, New York.
- Zhou, Y., R. K. Varner, R. S. Russo, O. W. Wingenter, K. B. Haase, R. Talbot, and B. C. Sive (2005), Coastal water source of short-lived halocarbons in New England, *J. Geophys. Res.*, *110*, D21302, doi:10.1029/2004JD005603.

J. Chen, M. Chen, R. J. Griffin, H. Mao, B. Sive, and R. Talbot, Climate Change Research Center, Institute for the Study of Earth, Oceans, and Space, University of New Hampshire, Morse Hall, 39 College Road, Durham, NH 03824-3525, USA. (mchen@gust.sr.unh.edu)